Annales de la Société Scientifique de Bruxelles, T. 103, III-IV, pp. 149-181 (1989)

APPLICATIONS OF SECOND ORDER MCSCF ON ELECTRONIC STRUCTURES, REACTIONS AND SPECTRA OF MOLECULES

by

HANS ÅGREN
Institute of Quantum Chemistry
University of Uppsala
Box 518, S-75120, Uppsala, Sweden

HANS JØRGEN AA. JENSEN
TRYGVE HELGAKER and POUL JØRGENSEN
Department of Chemistry
University of Aarhus
DK-8000 Aarhus, Denmark

and

JEPPE OLSEN
Department of Theoretical Chemistry
Chemical Centre
Box 714, S-22007, Lund, Sweden

ABSTRACT

The development and status of the second order MCSCF program package SIRIUS/ABACUS is briefly reviewed. A few applications illustrating the performance for calculations of electronic structures, reactions and spectra of molecules are discussed.

1. INTRODUCTION

The last decade has seen a rapid development of theory and code implementation of electronic structure methods in general and of methods for solving the many-body problem for molecules in particular. Although this development also today constitutes

an ever ongoing process, one can safely say that the theoretical endeavor in electronic structure methodology in the last few years has taken new turns and is now more directed towards accurate and efficient calculations of molecular properties. Particular emphasis has been put on the use of analytical response theory that makes the inherent accuracy of the electronic structure methods directly « transferable » to a number of molecular properties. This goes for many of the variational as well as perturbational methods in operation today, such as self-consistent field, configuration interaction, multiconfiguration self-consistent field, many-body perturbation theory, and coupled cluster methods (SCF, CI, MCSCF, MBPT, and CC). One of the more important properties in this respect are molecular derivatives, which form the underlying entities for the calculation of molecular conformations and reactions.

New formulations of response function theory, in conjunction with unitary parametrization of the wave function including also its time dependence, and the full use of second quantization has lead to a number of efficient approaches and simplifications that have been utilized for large scale calculations of molecular properties, as will be briefly sketched below. We have developed an MCSCF (Multi-Configurational Self-Consistent Field) method for this purpose. The main MCSCF code block implements a mathematically well-defined procedure for wave function optimizations which is analytically transferable to a number of properties as desired. This means that both computationally and formally the structure in this program part is similar to those for the different response property parts, in some cases the operations are identical. Being fully variational (in both configurational and orbital rotational parameters) the MCSCF wave function lends itselfs very well for use as reference in static of dynamic response property calculations. Perhaps the most important feature of the MCSCF model is, however, that it dissociates correctly, a property which stems from its inherent self-adjustable character that can handle *a priori* unknown electronic structures. In particular the making or breaking of molecular bonds and the description of electronic structures at transition states constitute problematic aspects in perturbational approaches but are handled correctly by MCSCF. In such cases

there is often a sharp variation of density and wave function, the latter containing mixture of covalent and ionic terms and near-degeneracies of electronic configurations etc. MCSCF thus starts out with a correct treatment of the static part of the electronic correlation and can gradually be enlarged to encompass the dynamical correlation. Some very recent work has indeed been concerned with the inclusion of a larger fraction of the dynamical correlation in MCSCF. The flexibility of the MCSCF model is particularly important for searches on a potential hypersurface away from equilibria, e.g. for transition states, where very little is known *a priori* about conformational or electronic structures.

The attractive features of MCSCF can thus be coined as « analytically transferable », « self-adjustable », « varational », and « general » in terms of transition and excited states. As shown in next paragraphs the inherent potential of MCSCF is fully utilized in a second order formulation. On the negative side one can mention lack of size-consistency, complex programming and calculations, and the fact that the non-linear optimization effectively prohibits a lack-box implementation, which is drawback in most, albeit not all, situations. Concerning the size-consistency problem one finds that the MCSCF wave function behaves better than the corresponding CI due to the orbital reoptimization, and one should also qualify its relative merits in this respect by the fact that at this time no computational feasible method is available that treats correctly both dissociation and size-consistency.

In this talk I will briefly review features and performances of a Multi-Configurational Self-Consistent Field method for calculating electronic structures, spectra, and reactions. The project started late 1983, and has resulted in a number of investigations published in the literature ; some key references are given in the reference list /1-32/. The program is parametrized for complete active (CAS) and restricted active (RAS) space wave functions using either a determinant based or a CSF (configuration state function) based many-electron basis. The program package contains four main modules :

i) SIRIUS : A direct second order MCSCF program. It is equipped with norm extended (NEO) and Newton-Raphson (NR) optimization routines using the trust region concept for guaranteed convergence, and also several auxiliary algo-

rithms for efficient optimization. It also includes a module for MC self-consistent reaction field calculations for a molecule or a cluster of molecules in a dielectric cavity.

ii) ABACUS : a second order property program for molecular gradients and Hessians, polarizabilities, IR intensities and frequencies. It is equipped with algorithms for searches of equilibrium and stationary points. Recently also incorporating routines for solving the equations of motions and autocorrelation functions for time development of ground and excited states.

iii) RESPONS : solves large eigenvalue equations and sets of linear equations for the linear time-dependent response functions of an MCSCF reference state. Dipole excitation spectra, dispersion coefficients, static and dynamic polarizabilities are obtained.

iv) WESTA : A program for transition properties and spectra obtained by separate state MCSCF optimization. It includes static and dynamic non-adiabatic (vibronic) coupling, X-ray and VUV spectra, and also core electron shake-up spectra.

The programs interface at present to three programs for calculation of one- and two-electron integrals : MOLECULE [33], HERMIT [34] and STOCOS [35], the two former ones using multicenter gaussian functions, the latter using one-center oscillating type (Slater + trigonometric) type functions.

2. SIRIUS

The primary MCSCF program for wave functions optimizations reviewed in this article can be attributed with three main labels ; i) second order ; ii) direct ; and iii) step-restricted. It is second order because it is based on the second-order Taylor expansion of the electronic energy in all variational parameters, viz. configuration coefficients and orbital rotations, which in turn imply quadratic convergence. It is direct because it gives the solution of an MCSCF eigenvalue equation by means of successive linear transformations where the full norm-extended Hessian is multiplied by a trial vector without explicitly constructing the Hessian. This makes possible applications to large wave functions for which the Hessian would be prohibitly large

for an explicit construction. The program is step-restricted because it performs a controlled walk on the energy hypersurface in which each step is restricted to a closed region, a hypersphere. The size of the latter is updated such that convergence is guaranteed for the lowest state of a given symmetry, and most often well-behaved for the lowest excited states. Thus the novel feature with the present MCSCF method, as implemented in the SIRIUS program was that it unifies two important developments in computational quantum chemistry ; the unitarily parametrized and density matrix driven second order MCSCF and the « CSF » (GUGA) or determinant based formulations for handling long configurational expansions. This makes it possible to handle large, and therefore accurate wave functions in a second order manner. The latter feature gives the possibility to obtain sharp and controllable convergence in relatively few number of iterations on the energy hypersurface, however, more important is that it offers analytical as well as computational advantages for property calculations, such as the molecular Hessians and other second order properties. A realization of this has been made in the ABACUS and RESPONS post-programs briefly commented below.

The following convergence characteristics are associated to the program

a) Guaranteed ground state convergence.

b) Reliable convergence for the lowest excited states.

c) Guaranteed correct state convergence (correct Hessian index).

d) Sharp convergence (for properties).

e) Root flipping problem avoided.

f) Core hole state convergence without variational collapse.

The basic assumption behind the MCSCF method is that of a spin-independent, Born-Oppenheimer Hamiltonian

$$\hat{H} = \Sigma_{rs} h_{rs} \hat{E}_{rs} + \frac{1}{2} \Sigma_{rstu} (rs \mid tu) \hat{e}_{rstu} \qquad (1)$$

where $\hat{E}_{rs}$ and $\hat{e}_{rstu}$ are the spin-less one- and two-electron excitation operators. The MCSCF wave functions is parametrized as

$$\Psi(q\,;\,Q) = exp(-\hat{\kappa})(\Sigma c_i \mid \Theta_i > \qquad (2)$$

where $\hat{\kappa} = \Sigma_{r>s} \kappa_{sr}(\hat{E}_{sr} - \hat{E}_{rs})$ is an asymmetric operator for orthogonal rotations of orbitals, and

$$| \Theta_i > = \hat{P} \prod_{\kappa=1,N} \hat{a}^+_{\kappa\sigma} \; | vac > \tag{3}$$

$$| \Theta_i > = \prod_{\kappa=1,N} \hat{a}^+_{\kappa\sigma} \; | vac > \tag{4}$$

denote configurational State Function (CSF) or Slater Determinant (SD) many-electron basis sets. The CSF:s thus constitute a spin-adapted SD basis. Each SD is constructed from a finite set of orthonormal orbitals $\varphi_i(q\,;Q)$, Molecular Orbitals (MO:s), which are expanded as linear combinations of atomic functions (LCAO) centered on the nuclei at Q :

$$\varphi_i(q\,;Q) = \sum_{\kappa} \; d^i_\kappa \xi_\kappa(q\,;Q) \tag{5}$$

The wave function expansion is thus (CSF)-SD-MO-LCAO with typical dimensions : CSF : $10^4 - 10^5$, SD : $10^5 - 10^6$, κ : $10^2 - 10^3$, or larger. The MCSCF wave function is obtained by optimizing the energy functional (suppressing Q-dependence) $E(\kappa, c) = E(x) = \frac{< 0 | \hat{H} | 0 >}{< 0 | 0 >}$, $| 0 > = | \Psi(x) >$, $x = (c,\kappa)$. For the stationary point X the energy gradient is zero and the energy Hessian has the correct index (0 for ground state, 1 for first excited state, etc.)

The wave function optimization can be thought of in two levels : i) a macro-iteration walk on the parameter surface towards the desired stationary point, and ii) the micro-iteration solution of a specific eigenvector-eigenvalue probleme which gives the optimal step for each macro-iteration. In order to take a macro step the energy surface is Taylor expanded around a given point

$$\delta E^2(\overline{y}) = \overline{g}^T \overline{y} + \frac{1}{2} \overline{y}^T \mathrm{H}' \overline{y} = \delta E(\overline{y}) + R^2(y) \tag{6}$$

the r.h.s. of which is divided into an exact energy difference for the step and a remainder energy. Only norm extended steps are considered (NEO) and the norm related variable is therefore projected out : $\overline{g} = \mathbf{P}\overline{g}$, $\mathbf{H}' = \mathbf{PHP}$, $\mathbf{P} = \mathbf{I} - \overline{x}\overline{x}^T$. Optimization of the quadratic function δE^2 gives

$$\overline{y}^N = -\mathbf{H}'^{-1} g \tag{7}$$

a straight Newton step, or

$$\overline{y}^R = -(\mathbf{H}' - \nu\mathbf{I})^{-1}g \tag{8}$$

a restricted, level-shifted step. Considering instead the eigenvalue equation

$${}^{\beta}\mathbf{L}\,{}^{\beta}\overline{z} = {}^{\beta}\lambda\overline{z} \tag{9}$$

where ${}^{\beta}\mathbf{L}$ is the projected and level-shifted Hessian

$${}^{\beta}\mathbf{L} = \mathbf{H}' + \beta(\overline{g}\overline{x}^T + \overline{x}\overline{g}^T) \tag{10}$$

one can find a step based on the eigenvector ${}^{\beta}\overline{z}$

$${}^{\beta}\overline{y} = (\beta(\overline{x}^T\,{}^{\beta}\overline{z}))^{-1}\mathbf{P}\,{}^{\beta}\overline{z} \tag{11}$$

that is equivalent to the restricted step

$$\overline{y}^R = -(\mathbf{H}' - {}^{\beta}\lambda\mathbf{I})^{-1}g \tag{12}$$

i.e. to a level-shifted Newton step. This scheme may be implemented such that it guarantees that the level shift always will lie in the correct interval. Solving for the restricted step (eq. (8)) as a set of linear equations would require calculations of the lowest eigenvalues of the Hessian beforehand in order to find the valid range for the level shift, while in the NEO approach the number of negative eigenvalues of the projected Hessian $\mathbf{H}'$ is monitored without ever explicitly determining any of its eigenvalues. With NEO one therefore automatically finds a level shift so that an optimal step can be taken. A non-linear algorithm has been set up to give a level shift such that the step is optimal for a trust region [36], i.e. a region where second order steps can be trusted. If the stationary point is outside the trust region a NEO step, i.e. solution of eq. (9), is taken with a level shift optimal for the current trust radius; if the stationary point is inside the trust radius, i.e. if the calculation has reached the local quadratic energy region, strict Newton-Raphson step(s) are taken towards the stationary point. A trust region update algorithm based on the ratio of predicted and actual energy changes is implemented such that convergence is guaranteed.

A typical second order MCSCF calculation thus proceeds by performing NEO type iteration steps on the global part of the energy hypersurface, while in the local energy region, where the surface is nearly quadratic and where the stationary point resides within the trust radius, a straight NR step is taken. For inner shell states one finds particularly nice applications of this procedure. These states are embedded in a continuum with an *a priori* unknown number of negative Hessian eigenvalues, and are subject to variational collapse. Full optimization can, however, be achieved by first carrying out an intermediate NEO optimization where the singly occupied core orbital is frozen which carries the expansion point to the local energy region, and then followed by a full optimization NR step without monitoring the Hessian index.

The step controlled pure second order character is one corner stone in the SIRIUS MCSCF program, the other novel feature in the program is its direct character, i.e. that the optimization step is solved for iteratively by evaluating linear transformations on trial vectors without explicitely constructing the generating matrix, *in casu*, the Hessian. We illustrate this step by splitting up the trial and updated vectors and the transformation matrices in orbital (o) and configurational (c) parts :

$$\begin{pmatrix} \overline{\sigma}^c \\ \overline{\sigma}^o \end{pmatrix} = \begin{pmatrix} {}^{\beta}\mathbf{L}^{cc} & {}^{\beta}\mathbf{L}^{co} \\ {}^{\beta}\mathbf{L}^{oc} & {}^{\beta}\mathbf{L}^{oo} \end{pmatrix} \begin{pmatrix} \overline{b}^c \\ \overline{b}^o \end{pmatrix} \tag{13}$$

We can view direct second order MCSCF as generalization to cases where

$${}^{\beta}\mathbf{L}^{co} = {}^{\beta}\mathbf{L}^{oc} = 0 \tag{14}$$

$${}^{\beta}\mathbf{L}^{oo} = {}^{\beta}\mathbf{L}^{co} = {}^{\beta}\mathbf{L}^{oc} = 0 \tag{15}$$

$${}^{\beta}\mathbf{L}^{cc} = {}^{\beta}\mathbf{L}^{co} = {}^{\beta}\mathbf{L}^{oc} = 0 \tag{16}$$

i.e. to first order MCSCF, direct configuration interaction, and to quadratic Hartree-Fock, respectively. In fact the program can be used for quadratically convergent step-restricted Hartree-Fock calculations, and is in this respect equivalent to the QC SCF method (quadratically convergent SCF) of Backskay [37] but with

the additional benefit of restricted step control. This direct (direct in terms of iterative solutions of the eigenvalue problem) HF has now been merged [38] with the direct (direct in terms of integral handling) SCF method of Almlöf and coworkers [39]. The MCSCF program can also be used straightforwardly for large scale direct CI calculations.

It is instructive to expand the above short form for the linear transformation somewhat for the different blocks :

$$cc{:}\sum_j {}^{\beta}\mathbf{L}^{cc}_{ij}b_j = 2(<\Phi^i \mid \hat{H} \mid B> - Eb_i) + (\beta - 1)[c_i(\sum_j g_j b_j) + g_i(\sum_j c_j b_j)] \qquad (17a)$$

$$oc{:}\sum_j {}^{\beta}\mathbf{L}^{co}_{sr,j}b_j = {}^{T}g_{sr} + (\beta - 2)g_{sr}\sum_j c_j b_j \qquad (17b)$$

$$co{:}\sum_{r>s} {}^{\beta}\mathbf{L}^{co}_{i,sr}b_{sr} = 2<\Phi_i \mid \overline{H} \mid MC> + (\beta - 2)c_i \sum_{r>s} g_{sr}b_{sr} \qquad (17c)$$

$$oo{:}\sum_{t>u} {}^{\beta}\mathbf{L}^{oo}_{sr,ut}b_{ut} = \overline{g}_{sr} + \frac{1}{2}\sum_t (b_{rt}g_{ts} - b_{st}g_{tr}) \qquad (17d)$$

In these equations i,j.. are configurational indices, $r,s,t,u..$ orbital indices. One can observe that only gradient like expressions appear and need to be stored, while Hessian elements do not appear explicitly, but are just multiplied onto the trial vector elements. The equations (17*c*) and (17*d*) thus express a direct operation with one-index transformed integrals, while equation (17*b*) represents a transition density matrix direct CI construction. The recognition of a one-index transformed Hamiltonian $\overline{H} = [\Sigma_{r>s}\, b_{sr}(\hat{E}_{sr} - \hat{E}_{rs}), \hat{H}]$ in the treatment of the coupling block [40] is a key point in the formulation of a second order MCSCF, in fact it is indispensable for a direct handling of the coupling block. In equation (17*c*) we note the appearance of ${}^{T}g_{sr}$ i.e. an orbital gradient evaluated from a second order transition density matrix. All expressions above are expanded and coded in terms of normal and transition 1- and 2- electron density matrices, normal 1-index transformed integrals and normal and one-index transformed and transition Fock matrices. All quantities are further subdivided according to if the orbital indices fall in the inactive, active or secondary categories, and in combinations of these categories.

As illustrated by eq:s (3) and (4) the MCSCF wave function is parametrized in both determinants and configuration state functions (CSF:s). The determinant expansions are typically 2 to 4 times longer than the CSF expansions, but make it possible to construct density matrices and sigma vectors more efficiently using vector operations. In some circumstances it is still advantageous to keep a purely spin-adapted CSF expansion, and the present version of the program therefore contains routines that make it possible to flip between determinant and CSF expansions in different parts of the program. The determinant expansion also makes the wave functions more readily manipulated in terms of annihilator or creator operations needed for matrix element calculations for interpreting various spectroscopic processes, see further section V.

The MCSCF wave functions are constructed in terms of Restricted Active Space (RAS) or of Complete Active Space (CAS) expansions. Despite this notion the RAS type wave function, introduced in CI by Olsen *et al.* [41], gives a possibility to obtain a major portion of the dynamic correlation energy, which is hard to reach with CAS expansions for all but the smallest one-particle basis sets, since the CAS wave function grows very rapidly with the number of active orbitals. The CAS wave functions are characterized by an orbital division into inactive, active and secondary spaces, which are doubly, fractionally and non-occupied, respectively. The inactive orbitals are optimized but not correlated; the active orbitals constitute the space for all possible electronic distributions that fulfill space and spin (for CSF:s) requirements, and are thus both correlated and optimized. In the RAS wave function the active space is further subdivided into three spaces, only one of which, RAS2, retains a complete character; the RAS1 space is specified by maximum number of holes, while RAS3 is specified by a maximum number of particles. The distribution of electrons in the RAS2 space is then determined by the conservation of the total number of active (correlated) electrons in the system. The choice of orbital division and also starting orbitals can be made by precalculations with MP2, CI or iterative natural orbitals CI (INO-CI) routines. The optimization of orbitals with small occupation numbers in the RAS3 space calls for natural or pseudo-natural transforma-

tions between iterations. Still, convergence can be slow in these cases, and this performance calls for some future improvements. It should be noted that RAS SCF has also been implemented for first order MCSCF in CSF basis by Malmquist *et al.* [42].

The program is also equipped with auxiliary algorithms to speed up convergence. These can be summarized as :

a) Improved start guesses for orbitals and wave functions given by HF, MP2, CI or INO-CI initial calculations.
b) Orbital absorption steps for fixed CI vectors.
c) A split Davidson algorithm.
d) Optimal orbital trial vectors.
e) Transform CI vector according to natural (CAS) or pseudo-natural orbitals (RAS) in between macro iterations.
f) Explicit construction of important parts of the CI Hamiltonian matrix to generate better trial vectors for the Davidson-Liu algorithm.

Some of the main data from a large CAS calculation using features *a*) to *e*) are recapitulated in Table 1. We find that a full

TABLE 1

Convergence characteristics for large MCSCF calculation of H_2O. $E - E^{conv}$ is the difference in atomic units between the total energy at the present step and at convergence. The figure in parentheses denote the number of CSF and orbital trial vectors in each macroiteration. Details of calculation are given in ref. 11.

Macroiteration	$E - E^{conv}$	step length
1	0.044 814 647 0 (2.2)	0.294
2	0.000 886 900 8 (3,3)	$3.40\ 10^{-2}$
3	0.000 000 361 7 (7,6)	$1.90\ 10^{-3}$
4	0.0	

MCSCF calculation requires only 12 direct sigma type operations, which is only slightly larger than the 9 iterations that the corresponding pure CI with the same wave function requires. With the use of feature f) (not yet applied) we expect to cut the number of sigma operations by a factor of two, in both the CI and the

MCSCF. For large orbital spaces also the number of integral transformations corresponding to the absorption steps (different transformation levels for different absorption levels) should be considered and especially the second-order integral transformation at each macro iteration will form a bottleneck. However, even if a second order integral transformation is more expensive than the corresponding first order one, the computational cost is substantially cut down with the number of macro iterations by using the potential of the auxiliary algorithms in second order MCSCF optimization, as is demonstrated by the few, here 3, macro iteration steps in the example of Table 1.

Based on the MCSCF method described above, we have recently worked out a new approach for studying solvent effects ; the multiconfigurational self-consistent reaction-field method, MCSCRF [17]. In this approach the atom, molecule or supermolecule is assumed to be surrounded by a homogeneous continuous medium described by its macroscopic dielectric constant. The MCSCF wave function for the solute molecule is fully optimized with respect to all variational parameters in the presence of the polarizable medium ; the optimization retains a pure second order character even with this interaction taken into account. A general algorithm for solvent integrals in terms of Hermite type Gaussian functions was developed, which allows for an expansion of the solvent multipole interaction to any order. Applications have so far concerned studies of electronic spectra of solvated species [24,25].

The present MCSCF program has been used in a broad variety of contexts for calculation of electronic structures, spectra and reactions, for systems of sizes ranging from Li^- over cyclobutadiene and cytosine to molecular clusters in solution. The important function of the SIRIUS program is being the main program for the different property programs. These will be, very briefly, reviewed below.

3. ABACUS

Geometry optimization using molecular gradient or gradient and Hessian techniques constitutes an area in quantum chemistry on which much methodological development has been

focussed lately, and some programs have already been routinely used in this context. There were several motivations for the development of an MCSCF approach to the calculation of molecular gradients, Hessians and potential energy searches. One is the correct dissociation feature built into MCSCF, another stems from the fully variational character of the MCSCF wave function making it particularly suitable for analytical response theory. The use of second order MCSCF has further the advantage that both formally and computationally the various properties, time-dependent and time-independent, can be formulated by similar means. It has been possible to identify the formal analogies of external and internal perturbations, for example the effect on the electronic (MCSCF) wave functions of an electric field and that of an internal perturbation from a nuclear displacement. The use of response theory then makes it possible to simultaneously monitor both the static and dynamic responses of such perturbations. Another example of this is that the direct techniques developed for solving large linear equations in wave function optimization can be utilized for the various properties as well, making such calculations applicable for wave functions with a very large number of parameters, which previously only was applicable for energy optimizations. In order to illustrate this point we consider a molecular system as a function of a static electric field ϵ and the nuclear coordinates x. We express the first and second order properties in terms of derivatives of the MCSCF energy functional $W(\epsilon, x)$ with respect to ϵ and x. Differentiation with respect to the electric field is denoted by m and with respect to the nuclear coordinates by n :

$$W^{mn}(\epsilon, \mathrm{x}) = d^{m+n} W(\epsilon, \mathrm{x}) / d\epsilon^{m} d\mathrm{x}^{\mathrm{n}} \tag{18}$$

The first order properties are then given by

$$W^{10} = E^{10} \text{ (dipole moment)} \tag{19a}$$

$$W^{01} = E^{01} \text{ (molecular gradient)} \tag{19b}$$

while the second-order properties are expressed as

$$W^{20} = E^{20} + R^{20} = E^{20} - \overline{F}^{10} G^{-1} F^{10}$$
(polarizabilities) (20*a*)

$$W^{11} = E^{11} + R^{11} = E^{11} - \overline{F}^{10} G^{-1} F^{01}$$
(dipole derivatives) (20*b*)

$$W^{02} = E^{02} + R^{02} = E^{02} - \overline{F}^{10} G^{-1} F^{01}$$
(molecular Hessian) (20*c*)

where the arguments $\epsilon = 0$ and $x = x_0$ for the unperturbed system have been dropped for convenience. The notation in these expressions define

$$E^{mn} = < 0 \mid \hat{H}^{mn} \mid 0 > \tag{21a}$$

$$F^{mn} = < 0 \mid [\hat{T}, \hat{H}^{mn}] \mid 0 > \tag{21b}$$

$$G = < 0 \mid [\hat{T}, [\hat{T}, \hat{H}]] \mid 0 > \tag{21c}$$

where $\mid 0 >$ is the MCSCF state for the unperturbed system, $\hat{H}$ and $\hat{H}^{mn}$ are the ordinary or the m,n times differentiated Hamiltonian and $\hat{T}$ the MCSCF orbital- and state-rotation operators. Note that no differentiation of the electronic Hessian enters these equations. The first-order properties contain static Hellmann-Feynman like terms whereas the second-order properties contain both static and relaxation terms ($E^{20} = 0$ though). The important point here is that the relaxation part can simply be written as $R^{20} = \overline{\lambda}^{10} F^{10}$, $R^{11} = \overline{\lambda}^{10} F^{01} = \overline{\lambda}^{01} F^{10}$, and $R^{02} = \overline{\lambda}^{01} F^{01}$, respectively, where λ^{10} and λ^{01} are solution vectors to the response equations $G\overline{\lambda}^{10} = -F^{10}$ and $G\overline{\lambda}^{01} = -F^{01}$ for the electrical and geometrical perturbations, respectively. These are identical to the Newton-Raphson equations solved in the electronic MCSCF step, only the electronic MCSCF gradient is replaced by gradient expressions for the perturbation F.

The simple and efficient formulation of response property calculations using large and therefore accurate wave functions stems from the use in equations (21) of a second-quantized, field and geometry dependent Hamiltonian

$$\hat{H}(\epsilon,X) = \sum_{pq} [h_{pq}^{OMO}(X) + \epsilon \mathrm{M}_{pq}^{OMO}(X)]\hat{E}_{pq}$$

$$+ \frac{1}{2}\sum_{pqrs} g_{pqrs}^{OMO}(X)[\hat{E}_{pq}\hat{E}_{rs} - \delta_{rq}\hat{E}_{ps}] \qquad (22)$$

Here h, g and M denote the one- and two-electron integrals and dipole integrals, respectively. All the field and geometry dependencies are isolated to these integrals, while expectation values of the creation and annihilation operators contained in $\hat{H}$ are preserved at any geometry. The results of this is that the geometry dependence becomes independent of the particular kind of wave function that is used and that standard response theory can be applied as discussed above. The formulation of this Hamiltonian is made possible by extending the reference MCSCF state to other geometries by means of using symmetrically orthogonalized orbitals

$$\psi_p(X) = \sum_q [S^{-\frac{1}{2}}]_{pq}(X)\,\xi_q(X) \qquad (23)$$

where $S_{pq}(X) = < \xi_p(X) \mid \xi_q(X) >$ is the overlap of the original orbitals at X_0 with the unmodified molecular orbitals at geometry X. The non-differentiated Hamiltonian then contains integrals over unmodified MO:s, while geometry differentiation of the Hamiltonian, needed in the response equations is achieved by a corresponding differentiation of the integrals carried out by a series of one-index tranformations using the differentiated S as the transforming matrix. This procedure can be extended to higher order derivatives [43].

With the molecular gradient and Hessian at hand a broad range of applications is opened. Geometry minimizations are now standard and implemented in many quantum chemistry programs and will not be commented on here. Finding stationary points other than equilibrium structures (ES:s), i.e. transition states (TS:s), is on the other hand far from routine. Firstly, the gradient information is not sufficient to characterize the transition state. Secondly, as already mentioned, the determination of the often complex and in most cases *a priori* unknown electronic structure requires a high level electronic structure method. In most cases neither experiments, other calculations nor intuition can aid in designing the appropriate wave function.

For a complex molecular surface it may become difficult to define a trust region for which the Taylor expansion converges. However, with the Hessian information, apart from obtaining the index of the converged stationary point, one has the possibility to traverse the surface from one stationary point to another by means of a series of local expansions of the potential. As for wave function optimization the second-order expansion gives the possibility for trust radius optimization, and finding equilibrium points is thus very similar to finding the optimum wave function. For transition state searches the trust radius algorithm in conjunction with an algorithm for determining the gradient extremal constitutes a powerful procedure as recently shown by Jørgensen *et al.* [20]. The gradient extremal (GE) is defined as the set of points on a potential surface for which the gradient is an eigenvector of the Hessian ;$H(X)g(X) = \lambda(X)g(X)$. The GE is very useful for potential walks since ; i) there is at least one GE connecting a TS with an ES (or two ES:s) ; ii) the GE coincides with a normal mode at a stationary point (ES or TS) ; iii) the GE:s are locally defined. Thus being at a stationary point one always departs along a normal mode (eigenvector of the Hessian), at other points the GE on the second-order surface satisfies the equation

$$X(\alpha) = -PH^{-1}g + \alpha v \tag{24}$$

where v is the eigenvector of the mode being followed and

$$-P = 1 - vv^T \tag{25}$$

projects away components along v. The α parameter is chosen such that the step length is equal to the trust radius. If the stationary point is within the trust region a straight Newton step is taken. Ref. [12] reports the results of a series of transition state searches between the three isomers of diazene, and gives a few hints of the amount of insight that can be gained in small molecular reactions by means of transition state searches.

With the possibility to locally expand molecular potentials of any dimension one can also look for solutions of the Heisenberg's quantum equations of motions (EOM) for molecular rearrangement or dissociation processes, which in turn gives the

possibility to analyze time-dependent or time-resolved phenomena. Thus only local rather than global information is needed to follow the time development of an electronic state e.g. over a transition state or after an electronic transition. In the latter case one often finds the system with high potential energy at an *a priori* unknown and often rough part of the potential. An accompanying dissociation process leads to redistribution of energy into internal and external degrees of freedom, which in principle can be traced by solving the EOM. For bound potentials it is possible to use the local gradient and Hessian information to construct auto-correlation functions, which after Fourier transformation give the multidimensional vibronic spectra directly. The build-up of a spectrum can then be followed along a time-resolved reaction walk. The auto-correlation function

$$C_{\alpha\beta}(t,\, t_0) = < \varphi_\alpha(R,\, t_0) \mid \varphi_\beta(R,t) > \qquad (26)$$

describes the time evolution of the measure of overlap between molecular electronic-vibrational wave function $\varphi_\beta(R,t)$ at two different times. At t_0 there exists a prepared wave function for the excited state φ_β as an eigenfunction of the initial state Hamiltonian $\hat{H}_\alpha$ (for times prior to t_0), which redefined to absorb the electronic transition momentum operator, will evolve in time according to the time-dependent Schrödinger equation for the final state Hamiltonian $\hat{H}_\beta$. As shown by Cesar *et al.* [31] it can be solved in an EOM approach through the construction of a vibronic propagator. For bound state potentials the auto-correlation function shows oscillations with frequencies that closely correspond to the eigenvalues of the Hessians at equilibrium geometry of the molecular system. For unbound potentials one can localize the time for passing a transition state or another point, which gives the possibility to obtain a transition state spectrum or a pico-second spectrum through e.g. a polarization propagator. Distinct nuclear dynamic processes that occur on different kinds of potential energy surfaces can be treated within a unified formalism. As a special case the auto-correlation function can be employed in conjunction with the Hessian and gradient at selected points, especially the vertical and adiabatic points (stationary points of initial respectively final states) in order to calculate a vibronic profile. No sum-over-state analysis

is required and basis set expansion for the final state eigenfunctions are also avoided; the bottle-neck for constructing a vibronic spectrum of any dimensionality lies in the calculation of the molecular Hessian itself. The same formalism can also be used for emission type spectra, where short lifetimes of the intermediate state leads to lifetime-vibrational interference effects [44].

4. RESPONSE

Response functions describe the effect of an external or internal perturbation on a reference state. If the perturbation is varying with time, such as an oscillating electric field, the response functions describe the time-dependent or equivalently the frequency dependent response of the wave function. The simplest time-dependent response function model, which describes the response of an SCF state, is the so-called Random Phase Approximation (RPA), also called time-dependent Hartree-Fock, which has been used extensively in conjunction with calculation of transition properties, spectral frequencies and moments of atomic and molecular spectra. Response function methods have also been derived for more sophisticated electronic wave functions, such as for MCSCF [45,46] and coupled cluster [47] states but also using perturbation theory [48]. For MCSCF states both linear (MCLR) and non-linear response functions have been derived by Olsen and Jørgensen [3]. They used a unitary parametrization of the time dependence of the reference state and obtained the response functions by applying Ehrenfest's theorem to determine the time development of the unitary parameters through each order in the interaction operator. Formally the MCLR approach leads to results that fulfill gauge invariance and sum-rules in the limit of a complete one-electron basis. In a general form the response function is determined from an MCLR two-component eigenvalue equation [3]:

$$\left[\begin{pmatrix} A & B \\ B & A \end{pmatrix} - \lambda_j \begin{pmatrix} \Sigma & \Delta \\ -\Delta & -\Sigma \end{pmatrix}\right] \begin{pmatrix} {}^1X_j \\ {}^2X_j \end{pmatrix} = \begin{pmatrix} 0 \\ 0 \end{pmatrix} \tag{27}$$

A and B are Hessian type matrices and Σ and Δ are metric type matrices. In short form this can be written as the generalized eigenvalue equations

$$(E^{(2)} - \lambda_j S^{(2)})\, X_j = 0 \tag{28}$$

An iterative solution of eq. (28) requires i) linear tranformations with $E^{(2)}$ and $S^{(2)}$ as transformation matrices [18] :

$$\begin{pmatrix} {}^1u \\ {}^2u \end{pmatrix} = \begin{pmatrix} A & B \\ B & A \end{pmatrix} \begin{pmatrix} {}^1b \\ {}^2b \end{pmatrix},\ u = E^{(2)}b \tag{29}$$

$$\begin{pmatrix} {}^1m \\ {}^2m \end{pmatrix} = \begin{pmatrix} \Sigma & \Delta \\ -\Delta & -\Sigma \end{pmatrix} \begin{pmatrix} {}^1b \\ {}^2b \end{pmatrix},\ m = S^{(2)}b \tag{30}$$

and an algorithm that determines the few lowest eigenvalues using the linear transformations in eq. (29) and (30). Recently Olsen *et al.* [18] proposed an iterative algorithm to solve eq. (2) which employ the pair-wise structure of the LR eigenvalue equations. In this algorithm a basis of orthonormal trial vectors is employed on which the exact equations are expanded using only matrix times vector operations. This procedure can be vieuwed as a generalization of the Davidson-Liu algorithm for the symmetric eigenvalue problem, which was used for solving the ordinary MCSCF eigenvalue equations (eq. (9)). The paired trial vectors are split into orbital and CSF (or determinant) components

$$\mathrm{b} = \begin{bmatrix} \kappa \\ 0 \\ \kappa' \\ 0 \end{bmatrix}, \begin{bmatrix} 0 \\ S \\ 0 \\ S' \end{bmatrix} \tag{31}$$

As for the symmetric eigenvalue equation the time consuming part of the linear transformation in eq. (9) is allocated to the direct CI type iterations and to the construction of a transition density matrix.

For a second order property, i.e. the frequency dependent polarizability we solve the LR equations

$$(E^{(2)} - \lambda_j S^{(2)})X_j = V^{(1)} \tag{32}$$

where λ_j is the frequency of the external perturbation, X_j the solution vector, and $V^{(1)}$ the gradient type vector for the con-

sidered perturbation. The second order property value is simply obtained as $X_j \; V^{(1)}$.

The major advantage of the LR scheme sketched above is thus that it gives the possibility to apply MCLR response calculations to large wave functions with the same kind of stable convergence as for the « ordinary » Davidson-Liu algorithm used in the wave function optimization. The algorithm and the analogous algorithm for solving the LR sets of linear equations are both solely based on the two linear transformations in eq:s (29) and (30). The feasibility of this algorithm, just as for MCSCF, lies in the fact that the two matrices never are constructed explicitly. Due to the large dimensions of $10^5 - 10^6$ or larger, it is important to reduce the number of iterations as much as possible. This is achieved by keeping as many « important » trial vectors in core memory as possible, and by always adding pairs of trial vectors to the reduced space such that the reduced space matrices maintain the paired structure of the full matrices. This assures that the roots of the reduced equations monotonically converges to the ones of the full MCLR eigenvalue equations, and that complex roots are avoided in the reduced space. As for MCSCF a slow convergence in orbital space calls for the application of an optimal orbital trial vector algorithm. When solving the linear equations for frequency dependent properties it is economic to reuse trial vectors of one frequency at new frequencies. These and other measures for convergence improvements have been described in detail in the original work, ref. (18).

The present LR scheme is implemented for HF, CAS and RAS wave functions giving the RPA and MCLR approaches. It has been applied to several systems [19,21,23,28,29], viz. Li^-, CH^+, N_2, ethylene, benzene and cytosine. For smaller systems close to full CI results are obtained with correlated wave functions that are not prohibitly large. For larger systems even larger CAS reference wave function sometimes fail to pick up sufficient amounts of the dynamic electronic correlation and further extensions to RAS-MCLR has been called for. The RAS scheme gives the possibility to obtain flexible means to design wave functions for very accurate results, in principle an open-ended convergence towards the correct results, in practice, of course, the limitation

in computational power and code implementation puts an effective limit. This limit has, however, not yet been fully explored.

In order to illustrate the strength of the present MCLR approach we recapitulate and shortly discuss some of the main results for the smallest of the above-mentioned species, namely the static and dynamic polarizabilities of Li^-. Like other alkali atoms, lithium has a stable anion with a very low electron affinity. Its electronic structure is commonly described as a three-body system with two highly correlated electrons circulating a positive unit charge. This evidently simple but still remarkable electronic structure has prompted many theoretical investigations of both conventional and unconventional character. The polarizability is not known to date, and the calculations give wide spread results. The applied approaches fall into three categories, scattering, perturbational and variational types. In Table 2 we recapitulate some of the main results for the polarizability of the Li^- ion from these investigations and from the MCLR method sketched above [28]. Table 3 collects some

TABLE 2

Collection of results for static polarization of Li^-

Reference	Method	Value(a.u.)
Lamm et al [54]	close coupling	734
Moores and Norcross [55]	close coupling	832
Pouchan and Bishop [56]	CI	650+/−50
Canuto et al [57]	SCF(RPA)	1199
—"—	SOPPA	1020
—"—	MP2	1130
—"—	MP3	996
—"—	MP4	994
—"—	CCD-PPA	780
—"—	CCSD-PPA	539
—"—	CCSDT-PPA	547
Ågren et al [28]	MCLR 21/2	804.5
—"—	MCLR 42/2	803.9
—"—	Full CI	797.8
—"—	Estimate of exact	798+/−5

TABLE 3

Gaussian (G) and Slater (S) basis sets referred to in Table 4.

Designation	basis	ref.
GI	(15s,9p) − <10s,6p>	[57,58,59]
GII	(16s,10p) − <16s,10p>	[57,58,59]
GIII	(16s,12p,4d) − <16s,10p,4d>	[57,58,59]
SI	(10s,8p,5d,4f) − <10s,8p,5d,4f>	[60,61]
SII	(15s,13p,5d) − <15s,13p,5d>	
	s: n_k=1: exp.=4.7071,3.5,2.4803	[60]
	s: n_k=2: exp.=1.735/q, q=1,12	
	p: n_k=2: exp.=3.5/q q=1,12	
	d: see SI	[60]

TABLE 4

Static and dynamic (ω= 0.02 a.u.) polarizabilities of Li^- in dipole length form (a.u.).

Wavefunction		Static					Dynamic
Correlating orbitals	number of electrons	GI	GII	GIII	SI	SII	GIII
0	0(SCF)	1201.79	1199.02	1198.39	1215.05	1196.10	1057.58
2s, 2p	2	459.77	457.10	622.97	636.71	625.94	781.59
2−3s, 2p	2	646.13	638.79	804.49	799.03	805.60	1216.25
2−3s, 2p−3p	2	646.92	638.48	804.22	798.83	805.42	1215.37
1−4s, 2p	4	647.85	639.35	805.54	800.25	806.77	1217.69
1−4s, 2p−3p	4	648.89	640.30	803.89	798.46	804.92	1216.09
1−4s, 2p, 3d	4	—	—	—	799.27	—	—
Full CI	4	651.58	645.49	797.77	—	—	1208.1

computational results for various basis sets of different types and sizes, and for different wave functions. The basis sets were of gaussian, Slater, and a type that combines Slater and trigonometric functions, and numerical MCSCF were performed to calibrate the convergence of energies. Finally full CI was perfor-

med for some of the basis sets for calibration purpose. We also calculated the experimentally known photodetachment threshold, and checked the results with respect to gauge invariance and sum rules. For all these quantities we obtain values that converge to 1 % or better to the correct results. This gives us the position to abstract information and trustworthy results [28,29] also for the experimentally unknown polarizability and photodetachment spectra for this species. First of all the static polarizability converges to 798 au, a value which we regard to be accurate to within 1 %. The frequency dependent polarizabilities show similar convergence behavior with respect to wave function parameters, and rises monotonically from $\omega = 0$ to $\omega = 0.618$ eV. The computed photodetachment threshold. (= 0.615 eV experimentally). As seen in Table 2 the scattering type calculations (close-coupling) agrees better with our results than later elaborate quantum methods. It is particularly distressing that for an effective two-electron system like Li^- the perturbational oriented CC and fourth-order MBPT approaches give different values, which are off by more than 20 % of the correct value. However, with an MCSCF reference state we obtain close to the correct value for small expansions of the wave function, e.g. the GIII basis set results in Table 3 give polarizabilities of 622.97, 804.49, 803.89 and 797.77 for the [2s,2p], [2-3s,2p], [1-4s,2p] and full CI wave functions, respectively, while the corresponding wave functions comprise 4,7,321 and 1155396 determinants. We find that the RPA value is 50 % higher than the exact basis set results, but that inclusion of the $2s^2-2p^2$ resonance by correlating the two valence electrons with the 2s and 2p orbitals halves the SCF value. Including an additional 3s orbital that describes the radial correlation raises this value by a third. In fact, correlating only the two valence electrons with the 2s,3s, and 2p orbital space we obtain values that already lie within 1 % of the exact basis set results. This indicates that a pseudopotential approximation is justified for Li^-. In order to rationalize these findings we also computed the expectation values $< r >$ and $< r^2 >$ for different choices of active spaces with the numerical MCSCF program. For the Hartree-Fock state one obtains $< r > = 12.65$ a.u. and $< r^2 > = 88.17$ a.u. An MCSCF expansion only including the near-degenerate configurations contracts the electron cloud to

$< r > = 11.49$ a.u. and $< r^2 > = 67.54$ a.u. The expectation values for the larger MCSCF expansions are stable, for the [1s-4s,2p,3d] calculations one obtains $< r > = 11.80$ a.u. and $< r^2 > = 73.29$ a.u. These observations provide a rationalization for the trends of the polarizability calculations, since the more diffuse an electron cloud is the easier it can be polarized.

Finally, we present in fig. 1 also the computed photodetachment spectrum of Li^-, taken from ref. (29). Also for this property there have been several previous investigations, although the deviations have not been as striking as for the polarizability. In the language of moment theory the polarizability is only one, namely the second moment, in a series of moments that can be used to form the full continuous photodetachment spectrum. This construction was achieved by the Stieltjes imaging moment method. The results show clearly that the spectrum has a « shape » resonance in the near continuum, the features of which vary much between the MCLR and RPA approaches. These observations also explain the widely dif-

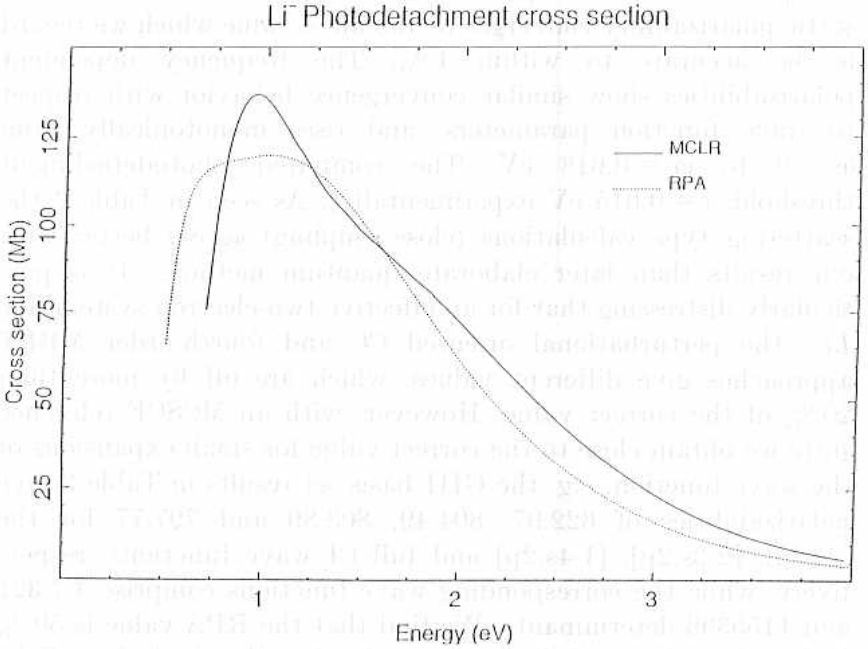

Figure 1. Photodetachment cross section of Li^- with RPA and MCLR methods [29].

ferent values for the polarizability, since this polarizability refers to the second moment of the cross section ; $\alpha = \int_{\omega_T}^{\infty} \frac{df(\omega)}{\omega^2}$; where ω_T is the detachment threshold. The sensitivity of the polarizability on the photoelectron spectrum closely above the detachment threshold, where ω is small and cross sections are large, thus explains also the quite different values obtained for this property by the RPA and MCLR methods. The structured low energy region is thus important, while the high energy region is unimportant for the polarizability, since the detachment cross sections become very small. The high-energy excitations make sizable contributions for an exact fulfillment of the zeroth order (Thomas-Reiche-Kuhn) sum rule, but thus not for the second order sum rule., i.e. for the polarizability.

In summary, we find that MCLR forms a very attractive approach for efficient and accurate calculations of time dependent and time-independent properties and spectra. This includes also calculations of photoelectron or photodetachment continua and shape resonances, as illustrated above for Li^-, since the primary excitation energies and moments directly can be used to construct the underlying moments and pseudospectra that are required to obtain a correctly energy normalized continuum. The MCLR program can be used as black box where the full spectrum is obtained in one batch of calculations. The ease of MCLR applications should thus be stressed.

5. WESTA

The third MCSCF post-program, WESTA, is coded for transition properties and spectra obtained from state specific optimizations of the wave functions. The WESTA program is divided into three parts. Part 1 evaluates generalized overlap amplitudes entering core photoelectron shake-up spectra or spectra from inverse photoemission. In part 2 X-ray transition moments are evaluated for VUV or X-ray spectra, i.e. spectra of processes which radiatively connect core and valence levels. Part 3 computes first and second order non-adiabatic coupling constants between seperately optimized MCSCF states. A numerical procedure with high inherent accuracy has been developed for this purpose. It has also been interfaced to an algo-

rithm for solving the coupled channel Schrödinger equation for which the non-adiabatic coupling constants enter as the basic input quantities. All three program units have been implemented for CAS wave functions, lately also for RAS although so far without any applications.

The two first parts of the program have in common that they treat spectral processes involving core levels. In comparison with theoretical analyses of spectra in the optical or UV wavelength region there are several additional considerations associated with studies of soft X-ray emission or core hole shake-up spectra. One of these refers to the fact that the initial state of the transition is embedded in a continuum and therefore may be subject to variational collapse. Also, the substantial electronic relaxation following the formation of the core hole introduces further complications. By virtue of the equivalent core notion, the transition takes place between two entirely different chemical species, which implies that the optimal molecular bases used for expanding the wave functions will be quite different for the initial and final states. This leads to a non-orthogonality problem in the evaluation of transition matrix elements between determinantal wave functions for both states. In a Hartree-Fock scheme this is manageable and has traditionally been solved by means of co-factor calculations. However, for correlated wave functions of even moderate accuracy such transition matrix elements require a large computational effort. Previous studies of molecular soft X-ray or core electron shake-up spectra have been carried out by means of self-consistent field and configuration interaction methods, and have shown that the orbital relaxation effect is crucial and that a correlated treatment of the transition matrix elements must always be performed separately for initial and final states with sets of mutually non-orthogonal orbitals. With independently optimized MO basis sets for the states involved one may account for the relaxation of the electronic cloud from the ΔSCF level and onward. However, the demand for state-specific MO optimizations puts an effective limit to the size of the wave functions that can be used in such calculations. Although some attempts have been made to attack these spectra with propagator oriented approaches, only state specific variational methods have been applied to any extent. The reason is

the difficulty to treat the large orbital relaxation and at the same time apply an operator manifold that contains core-valence transfer operators. Furthermore the core electron shake-up process is delicately dependent on the precise nature of the electron correlation, and would require higher order propagator methods if the unrelaxed ground state is used as reference state. On the other hand the state specific approaches to this kind of spectra have suffered from very costly evaluations of either the transition density matrix (soft X-ray emission) or wave function overlap (shake-up) when the wave functions are expanded in sets of mutually non-orthogonal sets of orbitals, and at the same time containing large configurational expansions. A « brute force » calculation of the matrix elements soon becomes prohibitive despite the application of some efficient schemes for co-factor calculations [49,50]. Overlap of the different wave functions are also needed to correct the transition moments for non-orthogonality.

The procedure for evaluationg the spectral moments

$$X_p^{(n)} = < \Psi_f^{(n)}(N-1) \mid \hat{a}_p \mid \Psi_i^{(0)}(N) > \tag{33}$$

$$X_p^{(n)} = < \Psi_f^{(n)}(N-1) \mid \hat{T} \mid \Psi_i^{(0)}(N-1) > \tag{34}$$

in the WESTA program are based on two parts ; i) an application of Malmquist's [51] biorthogonalization procedure ; and ii) algorithms for sorting and expanding the wave functions. This is implemented for both CAS and RAS wave functions either CSF or determinant based. For CSF:s the sorting and expansion is applied to the so-called GUGA graphs and to strings of determinants in the latter case. The need for these procedures stems from the single-occupancy restriction of the core hole, obtained by reducing the GUGA graphs (CSF:s) or restricting the RAS1 space to one electron only. This restriction is needed in order to avoid variational collapse, however, it still constitutes an excellent approximation to the full interaction, since interacting configurations with double core electron occupation are very small, below 0.1 eV as we have shown with perturbation theory [52]. Full orbital optimization can still be achieved with the MCSCF method as shown in section II. Using these proce-

dures we obtain timing for moment calculations that is completely negligible compared to that of the wave function optimizations. For X-ray spectra the spectral intensities are governed by the Einstein coefficients for spontaneous emission, which in Hartree units are given as

$$W_{ij} = \frac{4\alpha E_{ij}^3}{3c^2} T^2 \tag{35}$$

where c is the speed of light, α refers to the fine structure constant, E_{ij} denotes the transition energy, and T is the transition moment matrix element. The one-electron transition moment operator $\hat{T}$ is expressed in second quantization as

$$\hat{T} = \sum_{p,q} < \varphi_p^i \mid \hat{t} \mid \varphi_q^j > \hat{E}_{pq} \tag{36}$$

and the corresponding matrix elements as a trace of a property matrix multiplied by the first order density matrix.

$$\hat{T}_{ij} = \sum_{p,q} < \varphi_p^i \mid \hat{t} \mid \varphi_q^j > < \psi^i \mid \hat{E}_{pq} \mid \psi^j > = \sum_{p,q} P_{pq} D_{pq} \tag{37}$$

where ψ^i and ψ^j denote the total electronic wave functions for the initial and final state of the transition. We evaluate the transition moment either in dipole length or dipole velocity forms. These are related as

$$< \psi^i \nabla_r \mid \psi^j > = (E_j - E_i) < \psi^i \mid \hat{r} \mid \psi^j > \tag{38}$$

An efficient algorithm for calculating the property integrals is given in ref. (53). The construction of the transition density matrix follows Malmquist's prescription[ww] after that the wave functions for the « reduced » core hole state wave function has been expanded to a common « graph » used for the valence or ground state wave functions. Since separate MCSCF optimization of each state leads to non-orthogonality of the total wave functions and the magnitude of the transition moments may be of the same order of magnitude as the overlap between the MCSCF states, we have employed a symmetric orthogonalization procedure, $\mathbf{T}' = \mathbf{S}^{+\frac{1}{2}}\mathbf{T}$, to take care of this problem.

Applications have so far been carried out for some small molecules, see for example ref. (53) for X-ray emission and ref. (13) for shake-up spectra. Soft X-ray spectra of free

molecules pose some unusual and interesting features because of the combination of strict symmetry selection rules and effective, local, selection rules that govern their intensity distributions. Thus X-ray spectra « map » the valence electronic density of certain symmetries close to the initial state core hole. With the present method it has been possible to explore the role of different approximation levels from simple rules of thumb for frozen orbital one-center transition moments to the calculation of full transition moments using relaxed and correlated wave functions for all states involved. In the latter case gauge invariance within a few % has in general been obtained. The most crucial step seems to be that of the choice of orbitals. Due to the substantial electronic relaxation the intensities reflect a mixture of the initial and final states and the pertinent orbitals should ideally be evaluated separately. The ensuing non-orthoganality problem is thus alleviated by the present method. For molecular shake-up spectra electron correlation plays a decisive role. With large CAS SCF expansions one obtains a fair description of low-lying intensive shake up states, e.g. of first row diatomics, however, accurate results especially for higher lying shake-up peaks demand a very high quality of the wave functions for initial and final states including both static and dynamic kinds of correlation.

Finally, the third part of the WESTA program contains routines for calculation of first and second order non-adiabatic coupling constants and for the diagonal Born-Oppenheimer (BO) corrections. The break-down of the BO approximation is manifested in a number collisional and spectroscopic processes, and forms the underlying mechanism for charge transfer and for vibronic coupling and symmetry breaking. The present algorithm is based on numerical differentiation. The calculation of the first and second order non-adiabatic coupling elements

$$N_{ij}^{(1)}(Q^0) = \langle \Psi_i(q;Q) \mid \frac{\delta \Psi_j}{\delta Q}(q;Q) \rangle_{Q=Q_0} \tag{39}$$

$$N_{ij}^{(2)}(Q^0) = \langle \Psi_i(q;Q) \mid \frac{\delta^2 \Psi_j}{\delta Q^2}(q;Q) \rangle_{Q=Q_0} \tag{40}$$

is achieved by expanding the basic overlap element

$$K_{ij}(Q_0, x) = < \psi_i(q; Q_0 - x) \mid \psi_j(q; Q_0 + x) > \qquad (41)$$

symmetrically over the coupling point. This leads to one order higher accuracy than with a straight numeric differentiation, both for first and second derivatives. The coupling constants are then evaluated as

$$N_{ij}^{(1)}(Q_0) = (1/4x)*[K_{ij}(Q_0, x) - K_{ji}(Q_0, x)] + O(x^2) \qquad (42)$$

$$N_{ij}^{(2S)}(Q_0) = (1/4x)*[K_{ij}(Q_0, x) + K_{ji}(q_0, x)] - 2\delta_{ij}] + O(x^2) \qquad (43)$$

$$N_{ij}^{(2A)}(Q_0) = \frac{dN_{ij}^{(1)}}{dQ}(Q_0) = [N_{ij}^{(I)}(Q_0 + \frac{x}{2}) - N_{ij}^{(I)}(Q_0 - \frac{x}{2})/x + O(x^2) \qquad (44)$$

for the first, the symmetric and antisymmetric parts of the second order coupling constants, respectively. Symmetric orthogonalization is imposed on $\Psi_i(q,Q)$ and $\Psi_j(q,Q)$ which modulates the coupling constants by a simple scheme, see ref. (9).

Finalizing this section we briefly list a few applications [9,10,30] of the non-adiabatic coupling unit of the program : i) Calculation of non-adiabatic coupling constants for the ion-atom collison $Na + Li^+ \rightarrow Na^+ + Li$. This investigation included a close examination of the stability in the numerical procedure, sensitivity to electron correlation etc. : ii) Formulation of a diabatic model for photoionization with application to the much debated 27 eV structure in the photoelectron spectrum of acetylene. The first order non-adiabatic coupling constants are used to define the diabatic electronic states which diagonalize the nuclear kinetic operator instead of the electronic Hamiltonian. It was found that the diabatic representation was more appropriate than the adiabatic one for interpreting this spectrum : iii) The dynamic vibronic coupling between the $B^2\sum_u^+$ and $C^2\sum_g^+$ states of CO_2^+. Here spurious, probably symmetry forbidden, transitions are observed in the photoelectron spectrum. A conjecture was made that this is due to a vibronic coupling mechanism between the B and C states over the antisymmetric stretch motion. In order to prove this the vibronic spectra pertinent to

the dynamic non-Born-Oppenheimer potentials were calculated by solving the multichannel Schrödinger equation for the $B^2\sum_\mu^+$ and $C^2\sum_g^+$ ionic states, where the in-going first and second order non-adiabatic coupling constants as well as the Born-Oppenheimer potential surfaces were obtained from large CAS multi-configurational self-consistent field calculations. The results confirm the conjecture, however, although one finds qualitatively confirmation at the CAS level, the results are very sensitive to the computational procedure, and we envisage large scale RAS calculations as a requisite for obtaining converged quantitative results.

REFERENCES

[1] H.J. Aa. Jensen, and P. Jørgensen, *J. Chem. Phys.*, **80**, (1984), 1204.
[2] H.J. Aa. Jensen, and H. Ågren, *Chem. Phys. Letters*, **110**, (1984), 140.
[3] J. Olsen and P. Jørgensen, *J. Chem. Phys.*, **82**, (1985), 3235.
[4] H.J. Aa. Jensen, and H. Ågren, *Chem. Phys.*, **104**, (1986), 229.
[5] H.J. Aa. Jensen, P. Jørgensen and T.U. Helgaker, *J. Chem. Phys.*, **85**, (1986), 3917.
[6] T.U. Helgaker, H.J. Aa. Jensen, and P. Jørgensen, *J. Chem. Phys.*, **84**, (1986), 6280.
[7] T.U. Helgaker, J. Almlöf, H.J. Aa. Jensen, and P. Jørgensen, *J. Chem. Phys.*, **84**, (1986), 6266.
[8] H.J. Aa. Jensen, and H. Ågren, Documentation of SIRIUS, a general purpose direct second-order MCSCF program. Theory-, Input Reference-, and Program Reference Manuals, Technical notes 783, 784, and 785, Institute of Quantum Chemistry, University of Uppsala.
[9] H. Ågren, A. Flores-Riveros, and H.J. Aa. Jensen, *Phys. Rev.*, **A34**, (1986), 4606.
[10] A. Flores-Riveros, H. Ågren, R. Brammer, and H.J. Aa. Jensen, *J. Chem. Phys.*, **85**, (1986), 6270.
[11] H.J. Aa. Jensen, P. Jørgensen, and H. Ågren, *J. Chem. Phys.*, **87**, (1987), 451.
[12] H.J. Aa. Jensen, P. Jørgensen, and T.U. Helgaker, *J. Am. Chem. Soc.*, **109**, (1987), 2895.
[13] H. Ågren, and H.J. Aa. Jensen, *Chem. Phys. Letters*, **137**, (1987), 431.
[14] H.J. Aa. Jensen, P. Jørgensen, H. Ågren, and J. Olsen, *J. Chem. Phys.*, **88**, (1988), 3834.
[15] J. Olsen, B.O. Roos, P. Jørgensen, and H.J. Aa. Jensen, *J. Chem. Phys.*, **89**, (1988), 2185.
[16] T.U. Helgaker, and P. Jørgensen, *Adv. Quant. Chem.*, **19**, (1988), 183.
[17] K. Mikkelsen, H. Ågren, H.J. Aa. Jensen, and T.U. Helgaker, *J. Chem. Phys.*, **89**, (1988), 3086.

[18] J. Olsen, H.J. Aa. Jensen, and P. Jørgensen, *J. Comp. Phys.*, **74**, (1988), 265.
[19] H.J. Aa. Jensen, H. Koch, P. Jørgensen, and J. Olsen, *Chem. Phys.*, **119**, (1988), 297.
[20] P. Jørgensen, H.J. Aa. Jensen, and T.U. Helgaker, *Theor. Chim. Acta*, **73**, (1988), 55.
[21] P. Jørgensen, H.J. Aa. Jensen, and J. Olsen, *J. Chem. Phys.*, **89**, (1988), 3654.
[22] D. Nordfors, N. Mårtensson, and H. Ågren, *Phys. Rev.*,**B38**, (1988), 12922.
[23] J. Olsen, A.M. Sanchez de Meras, H.J. Aa. Jensen, and P. Jørgensen, *Chem. Phys. Letters*, **154**, (1989), 380.
[24] C. Medina-LLanos, H. Ågren, K. Mikkelsen, and H.J. Aa. Jensen, *J. Chem. Phys.*, **90**, (1989), 6422.
[25] H. Ågren, C. Medina-LLanos, K. Mikkelsen, and H.J. Aa. Jensen, *Chem. Phys. Letters*, **153**, (1989), 322.
[26] A. Cesar, H. Ågren, T.U. Helgaker, H.J. Aa. Jensen, and P. Jorgensen, in preparation.
[27] H. Ågren, A. Flores-Riveros, and H.J. Aa. Jensen, *Physica Scripta*, **40**, (1989), 745.
[28] H. Ågren, J. Olsen, H.J. Aa. Jensen, and P. Jørgensen, *Phys. Rev.*, **A40**, (1989), 2265.
[29] V. Carravetta, H. Ågren, H.J. Aa. Jensen, P. Jørgensen, and J. Olsen, *J. Phys.*, **B22**, (1989), 2133.
[30] M. Natiello, O. Vahtras, A. Engelmann, and H. Ågren, in manuscript.
[31] A. Cesar, H. Ågren, in preparation.
[32] H.J. Aa. Jensen, H. Ågren and J. Olsen, P. Jørgensen, *SIRIUS a general purpose direct second order program*, MOTECC-90, Ed. E. Clementi, Escom Science Publishers, 1990.
[33] J. Almlöf, *USIP*, nr. 74-29, University of Stockholm (1974).
[34] T. Helgaker, unpublished.
[35] I. Cacelli, V. Carrevetta, and R. Moccia, *Chem. Phys.*, **90**, (1984), 313.
[36] R. Fletcher, *practical methods of optimization*, Vol. 1 (Wiley, New York, 1980).
[37] G.B Bacskay, *Chem. Phys.*, **61**, (1980), 385.
[38] M. Feyereisen et al., unpublished.
[39] J. Almlöf, K. Faegri, and K. Korsell, *J. Comp. Chem.*, **3**, (1982), 385.
[40] J. Olsen, D. Yeager, and P. Jørgensen, *Advan. Chem. Phys.*, **54**, (1983), 1.
[41] J. Olsen, B.O. Roos, P. Jørgensen, and H.J. Aa. Jensen, *J. Chem. Phys.*, **89**, (1988), 2185.
[42] P. Å. Malmquist, A. Rendell and B.O. Roos, *J. Phys. Chem.*, (1990).
[43] J. Simons, P. Jørgensen, and T.U. Helgaker, *Chem. Phys.*, **79**, (1983), 334.
[44] A. Cesar, H. Ågren, and V. Carravetta, *Phys. Rev.*, **A40**, (1989), 187.
[45] D.L. Yeager and P. Jørgensen, *Chem. Phys. Letters*, **65**, (1979), 77.
[46] E. Dalgaard, *J. Chem. Phys.*, **72**, (1980), 816.
[47] E. Dalgaard and H.J. Monkhorst, *Phys. Rev.*, **A28**, (1983), 1217.

[48] J. Oddershede and P. Jørgensen, *J. Chem. Phys.*, **66**, (1977), 1541.
[49] F. Prosser, and S. Hagstrom, *Int. J. Quant. Chem.*, **2**, (1968), 89.
[50] H. Ågren, R. Arneberg, J. Müller, and R. Manne, *Chem. Phys.*, **83**, (1984), 53.
[51] P.Å. Malmquist, *Int. J. Quant. Chem.*, **30**, (1986), 479.
[52] V. Carravetta, H. Ågren, and A. Cesar, *Chem. Phys. Letters*, **148**, (1988), 210.
[53] H. Ågren, A. Flores-Riveros, and H.J. Aa. Jensen, *Physica Scripta*, **40**, (1989), 745.
[54] G. Lamm, A. Szabo, and S.A. Adelman, *Phys. Rev.*, **A17**, (1978), 238.
[55] D.L. Moores and D.W. Norcross, *Phys. Rev.*, **A10**, (1974), 1646.
[56] C. Pouchan and D.M. Bishop, *Phys. Rev.*, **A29**, (1984), 1.
[57] S. Canuto, W. Duch, J. Geertsen, F. Müller-Plathe, J. Oddershede, and G.E. Scuseria, *Chem. Phys. Letters*, **147**, (1988), 435.
[58] L. Gianiolio, R. Povani, and E. Clementi, *Gazz. Chim. Ital.*, **108**, (1978), 181.
[59] F.B. van Diujneveldt, *IBM Techn. Rept.*, (1971), RJ945.
[60] A.C. Fung and J.J. Matese, *Phys. Rev.*, **A5**, (1972), 2.
[61] C.F. Bunge, *Phys. Rev. Lett*, **44**, (1980), 1450 ; C.F. Bunge, *Phys. Rev.*, **A22**, (1980), 1.